Efficiency Impact of Silicon Carbide Power Electronics for Modern Wind Turbine Full Scale Frequency Converter

Hui Zhang, *Member, IEEE*, and Leon M. Tolbert, *Senior Member, IEEE*

***Abstract*—Power electronics is an enabling technology found in most renewable energy generation systems. Because of its superior voltage blocking capabilities and fast switching speeds, silicon carbide (SiC) power electronics are considered for use in power conversion units in wind generation systems in this paper. The potential efficiency gains from the use of SiC devices in a wind generation system are explored by simulations, with the system modeling explained in detail. The performance of the SiC converter is analyzed and compared to its silicon counterpart at different wind speeds, temperatures, and switching frequencies. The quantitative results are based on SiC metal–oxide–semiconductor field-effect transistor (MOSFET) prototypes from Cree and modern Si insulated-gate bipolar transistor (IGBT) products. A conclusion is drawn that the SiC converters can improve the wind system power conversion efficiency and can reduce the system's size and cost due to the low-loss, high-frequency, and high-temperature properties of SiC devices, even for one-for-one replacement for Si devices.**

***Index Terms*—Converter, modeling, metal–oxide–semiconductor field-effect transistor (MOSFET), silicon carbide (SiC), wind generation.**

I. Introduction

VARIABLE speed capability allows a wind turbine to operate at speeds which produce the greatest amount of power and minimizes torque perturbations in the drive train [1]–[5]. This capability tends to decrease the overall cost of energy because the amount of energy generated is increased and the cost of the drive train and its maintenance are reduced. Since the voltage and frequency of the generated power vary with the turbine speed, a converter is required to reconcile the output with the fixed voltage and frequency of the grid [6]–[10].

Several technical and market reports [11]–[13] have recognized silicon carbide (SiC) power electronics as a potential technology for wind turbine power converters. The primary benefits of SiC-based power devices include low losses, high temperature tolerance, and fast switching. These can be exploited to reduce generation losses and increase net energy production. The low losses, along with high temperature tolerance, can also be used to improve the reliability of the converter and reduce the thermal management requirements. Moreover, fast switching has the potential to reduce the filtering passive component size and cost, thus, the total cost of the system. Reference [13] provides a simulation for the efficiency performance of SiC-based converters that might be used in a wind turbine and it provides quantitative comparison with commonly used Si converters. This paper also provides quantitative results, but simulations have been updated by using experimentally tested characteristics of more recently developed SiC metal–oxide–semiconductor field-effect transistor (MOSFET) and Schottky diode device prototypes.

Manuscript received July 31, 2009; revised December 3, 2009 and February 16, 2010; accepted March 22, 2010. Date of publication April 29, 2010; date of current version December 10, 2010.

H. Zhang is with the Department of Electrical Engineering, Tuskegee University, Tuskegee, AL 36088 USA (e-mail: hzhang18@ieee.org).

L. M. Tolbert is with the Min Kao Department of Electrical Engineering and Computer Science, The University of Tennessee, Knoxville, TN 37996-2100 USA, and also with the Power Electronics and Electric Machinery Research Center, Oak Ridge National Laboratory (ORNL), Knoxville, TN 37932 USA (e-mail: tolbert@utk.edu).

Color versions of one or more of the figures in this paper are available online at http://ieeexplore.ieee.org.

Digital Object Identifier 10.1109/TIE.2010.2048292

II. Wind Turbine System and Modeling

A wind turbine system is designed based on the National Renewable Energy Laboratory's (NREL) baseline wind turbine described in [14]. It is composed of a 1.5 MW wind turbine, a permanent magnet (PM) generator rated at 690 V, a bidirectional full scale frequency converter comprised of two back-to-back inverters, and a utility filter (simplified as a single inductance), as shown in Fig. 1 [15]. The wind energy is converted to electricity by the PM generator and then transferred to the utility. In this process, the converter plays two roles: 1) to control the generator to capture as much wind energy as possible and 2) to deliver the energy to the utility. In both roles, the power loss in the converter is of utmost concern, which not only determines the design of the converter, but also affects the other components in the system, such as the filter. The converter efficiency will be demonstrated by the simulation results, and the effect of applying SiC devices on such a system is also analyzed. The associated modeling work will be presented in this section.

As shown in Fig. 2, the system modeling is composed of four models: wind turbine model, device model, converter model, and thermal model. The system inputs are input power, the speed of the generator, ambient temperature, and the switching frequency of the converter. The output will be the system efficiency. The four models are connected by parameters. For example, wind turbine and device models provide parameters for the converter model, and the output of the converter model is fed to the thermal model. Then, the junction temperature obtained from the thermal model is provided to the device model, which starts the next calculation step based on the new

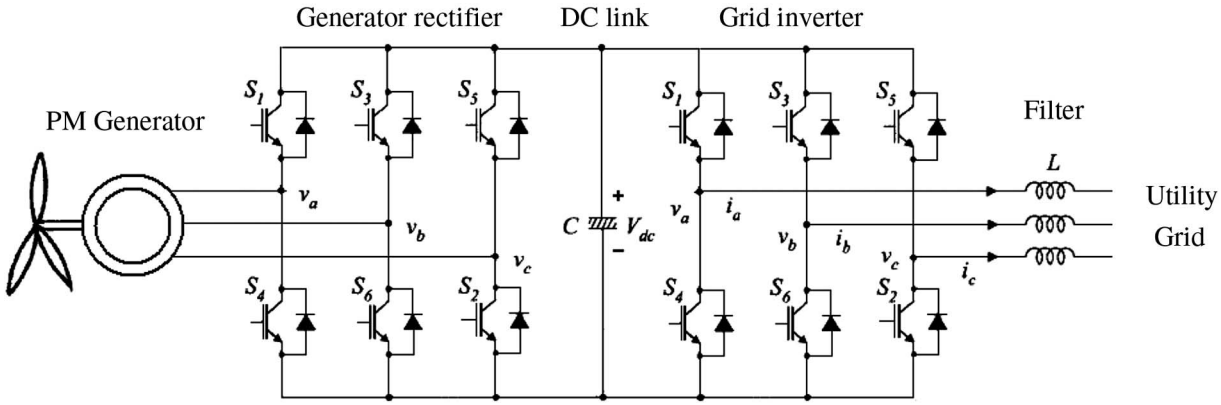

Fig. 1. Wind generation system structure with full scale converter.

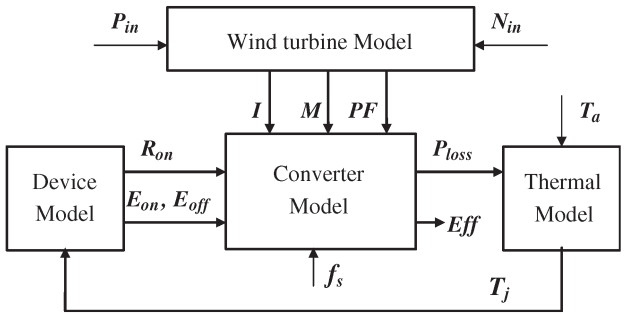

Fig. 2. System modeling diagram.

temperature information. Each model is explained in detail in the following sections.

A. Wind Turbine Model

The wind turbine model is mainly a PM generator model, whose function is to calculate the current, power factor, and the modulation index, which are needed by the converter model based on the input power and the speed of the generator. The electrical parameters of the generator studied in this work are listed in Table I. Assuming that the generator back electromotive force is in phase with the generator current, then a simplified PM generator model can be developed using a dq rotating coordinate system analysis. With this generator model, the output voltage and current of the generator can be obtained. They are also the ac side current and voltage of the rectifier in the back-to-back converter. Then, based on the relationship between the ac side and the dc voltage in an inverter with sinusoidal pulse width modulation (SPWM) technique, the modulation of the converter can be calculated. The full list of equations can be found in [13].

B. Device Models

Device models describe the device characteristics related to the operation losses. In this paper, they are look-up tables or polynomial functions based on the curve fitting of test results. Most recent SiC MOSFET prototypes were obtained and tested for both static and dynamic characteristics, which were then used for curve fitting.

TABLE I
WIND GENERATION SYSTEM PARAMETERS

Generator parameters	
Rated power, MW	1.5
Nominal voltage, V	690
Rated speed n_0, rpm	164
Back emf at n_0, Emf_0, V	150
Base machine pole number p	56
Stator phase resistance R, Ω	1.23e-2
Stator phase inductance L, H	6.62e-4
Eddy loss at n_0, P_{le0}, kW	4.284
Hysteresis loss at n_0, P_{lh0}, kW	1.848
Others	
DC link voltage V_{dc}, V	1100
Grid voltage V_{ll}, V	690
Grid power factor, cosϕ	0.95
filter loss constant, k	0.0097

TABLE II
DEVICES USED IN CONVERTERS

Item	Voltage rating	Current rating	Part number
SiC MOSFETs	1200V	10A×20×10	CREE, Prototype
SiC Schottky diodes	1200V	10A×20×10	CREE, C2D10120
Si IGBT/diode modules	1700V	1200 A×2	DYNEX, DIM1200FSM17

The prototype SiC MOSFETs listed in Table II were experimentally tested with a curve tracer at different ambient temperatures, from 25 °C to 300 °C, with an increment of 25 °C. As expected, the on-state resistances of the MOSFETs increase with temperature, as shown in Fig. 3(a). After scaling the rating of the SiC MOSFETs to 1700 V and 1200 A, which is the rating of the Si IGBTs used in this work (see Table II), not only the on-state resistance (0.76 mΩ at RT) of the SiC MOSFETs is smaller than that of the Si IGBTs (0.84 mΩ at RT), but also the change rate of the resistances with temperature is smaller. The on-state resistances of the SiC MOSFETs increase by 11.8% when temperature changes from room temperature to 125 °C, compared to 41.8% for the Si IGBTs. Thus, the SiC devices are more efficient in terms of having lower conduction loss, particularly at higher temperatures. The transfer characteristics of the MOSFETs in Fig. 3(b) change slightly with an increase

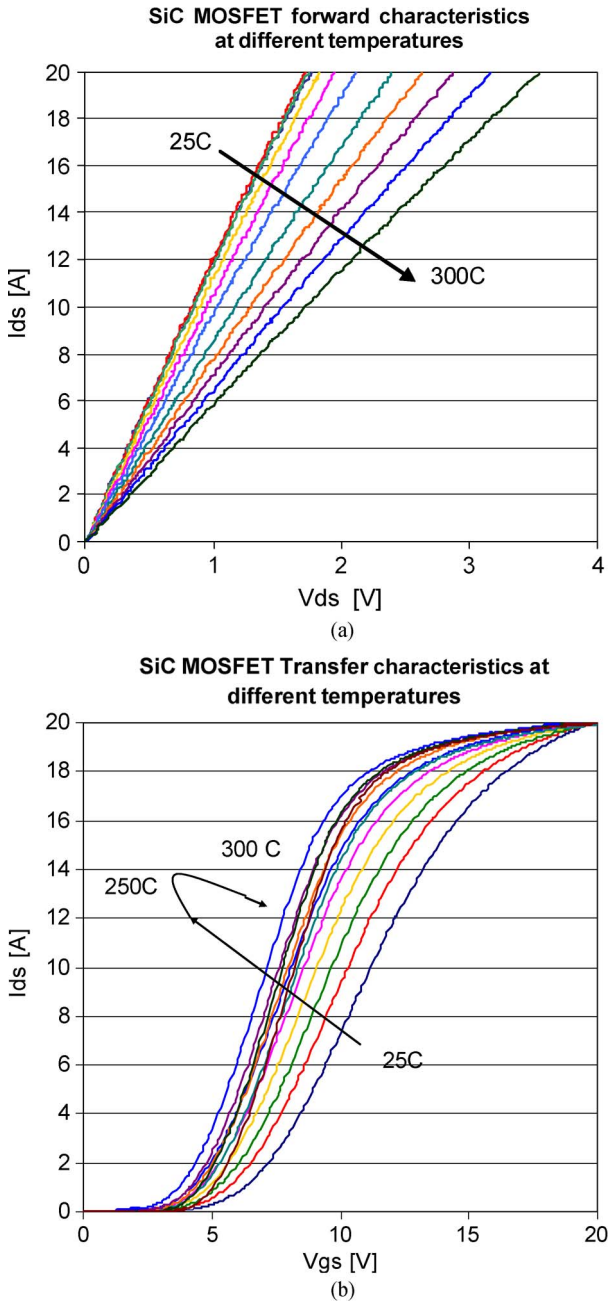

Fig. 3. Static characteristics of the SiC MOSFET at different temperatures. (a) Forward characteristics. (b) Transfer characteristics.

in temperatures above 150 °C. This indicates that the change in switching losses of the MOSFETs with temperature will be small. This is confirmed by the switching tests (Fig. 6).

The circuit shown in Fig. 4 is used to obtain the switching characteristics in Figs. 5 and 6. The ambient temperature of the SiC MOSFETs is varied from 25 °C to 225 °C, with an increment of 50 °C. With a pure inductive load, the current in the switches can be controlled by adjusting the duty ratio of the first pulse when applying a double-pulse control signal. Commercial gate driver IC HCNW3120 is selected to drive the SiC MOSFETs. It generates a voltage of about 20 V at turn-on and 0 V at turn-off. The gate drive board is separate from the MOSFET, and its ambient temperature is room temperature. As shown in Fig. 5, with a gate resistance of 10 Ω, the MOSFET

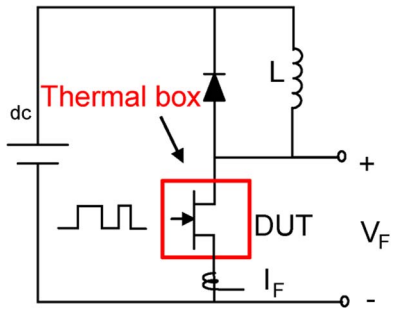

Fig. 4. Switching test circuit.

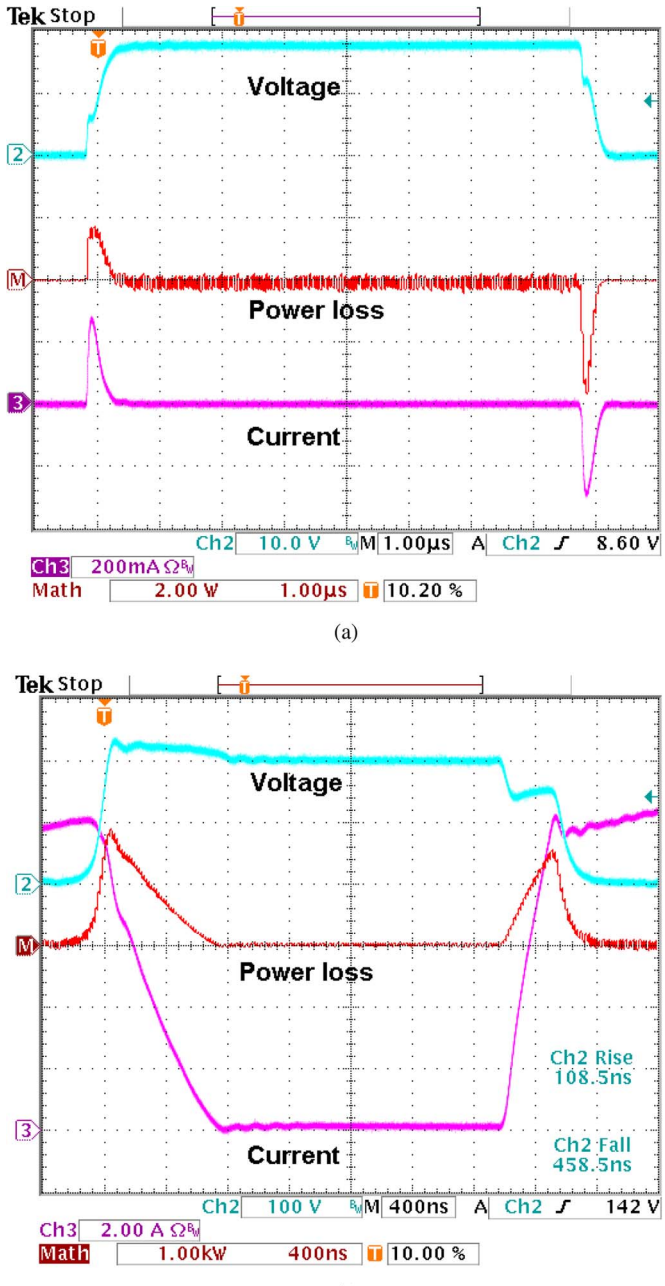

Fig. 5. Test waveforms of the SiC MOSFET (Cree) at 225 °C. (a) Gate signal waveforms. (b) Switching waveforms.

works functionally up to 225 °C ambient temperature at a power level of 200 V and 10 A. The peak gate current at this condition is 280 μA.

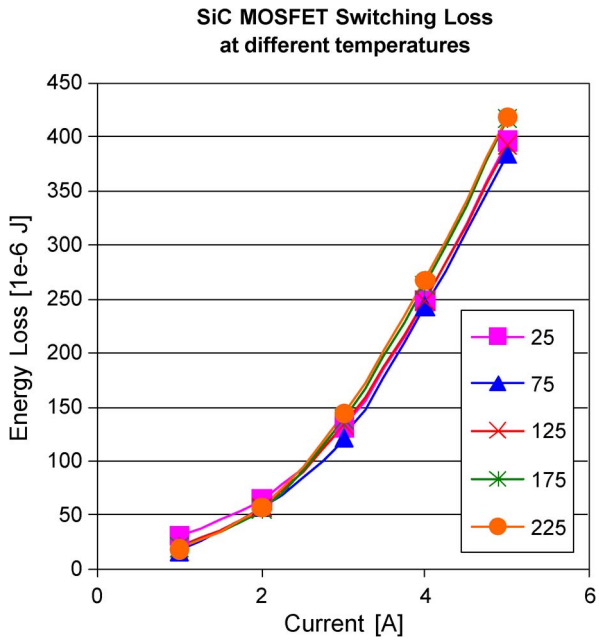

Fig. 6. Switching losses of the SiC MOSFET at different temperatures.

The switching losses, including both turn-on and turn-off losses, are calculated at each test condition. They are plotted versus the drain current at each tested temperature in Fig. 6. The switching losses increase as the current increases, but change very slightly when ambient temperature changes, while the increase of the switching losses of Si devices is much more obvious. For the Si IGBT used in the work, its switching loss increases by 56.3% when case temperature changes from 25 °C to 125 °C. Thus, the substitution of SiC devices for Si devices will improve system efficiency, and with higher temperature and higher switching frequency, the system will gain even more benefits compared to the Si-based system.

C. Converter

A 1.5 MW converter is required to provide full power conditioning for the full output of the generator. Because no SiC devices are presently available at this rating, the converter is assumed to be composed of ten SiC-based converters that each use twenty 10 A SiC MOSFETs for a power rating of 150 kW each in the simulation, which are based on the devices listed in Table II. The multiples in the current column mean the number of devices in parallel and the number of converters in parallel.

Similarly, Si IGBT/diode modules with maximum available ratings are selected to form a converter representing today's Si power electronic techniques. The Si modules are single-switch modules with two single IGBTs and two single diodes rated at 1200 A in parallel. To meet the power requirement for this application, two such Si converters will be needed in parallel.

In addition, with the improvement of current ratings for single SiC devices in the future, there will be no need to parallel so many more SiC devices than Si devices to achieve a module at the same power level. Presently, many research efforts have been made to improve the single-device rating and develop high-power modules [26]–[30]. The single SiC switch rating is up to 1200 V and 50 A [29]. The largest SiC power module reported in literature is 10 kV and 100 A [28]. There have also been 1200 V, 600 A phase-leg-module prototypes under development.

As high current rated SiC power devices and modules mature in their development, future SiC inverters will be comparable to the present Si IGBT inverters in terms of difficulty of paralleling devices and of complexity resulting from the additional components such as gate drivers, connectors, etc. This will enable the practical application of SiC inverters in such high-power systems as the wind turbine system discussed in this paper.

Because of the unavailability of such high-power SiC modules at present, the best prediction of what will be achievable when using SiC devices in the near future can be extracted from the characteristics of presently available devices. Two assumptions are made for this prediction: 1) future SiC devices will have the same performance as with today's SiC devices, and 2) module packaging technology does not introduce parasitics or issues other than those found in single device packaging. The first assumption is a conservative one, while the latter one is overly optimistic. Thus, actual performance will vary slightly from the predicted performance in future SiC inverters and will depend on the continued future device development and packaging technologies for large current rated SiC power electronic modules.

D. Power Loss Models

A widely used averaging technique [16]–[19] is employed to study the inverter power loss. This technique takes a sample from each switching cycle and then uses these values to find the effective value at the fundamental cycle of the output. The resultant equations are presented in the following paragraphs. In these equations where $\pm$ appears, the upper sign should be used for inverter calculations, and the bottom one is for rectifier calculations. More details are provided in [20] and [21].

For SiC MOSFETs, the conduction loss is caused by on-state resistance R_{on}. It is calculated by:

$$P_{M,cond} = I^2 R_{on,M} \left(\frac{1}{8} \pm \frac{1}{3\pi} M \cos\phi \right) \tag{1}$$

where M is the modulation index, I is the peak of phase current, and ϕ is the phase angle of the current with respect to voltage. For the SiC Schottky diode and Si IGBT, the voltage drop is not zero when the current is zero. Thus, there is an additional loss associated with this voltage drop V_0. Conductive loss equations are shown as (2) for the diode and (3) for the IGBT

$$P_{D,cond} = I^2 \cdot R_{on,D} \left(\frac{1}{8} \mp \frac{1}{3\pi} M \cos\phi \right) + I \cdot V_0 \cdot \left(\frac{1}{2\pi} \mp \frac{M \cos\phi}{8} \right) \tag{2}$$

$$P_{I,cond} = I^2 \cdot R_{on,I} \left(\frac{1}{8} \pm \frac{1}{3\pi} M \cos\phi \right) + I \cdot V_0 \cdot \left(\frac{1}{2\pi} \pm \frac{M \cos\phi}{8} \right). \tag{3}$$

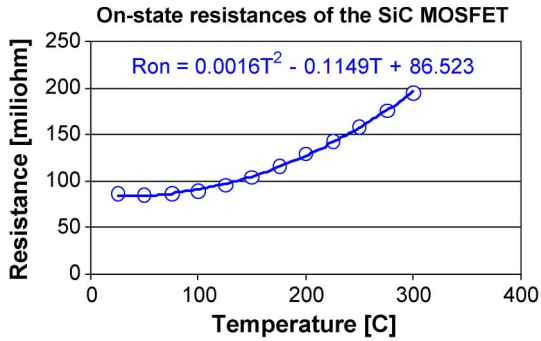

Fig. 7. On-state resistance of the SiC MOSFET.

The value of R_{on} for each device may change with current and temperature. Look-up tables or polynomial functions can be used to express R_{on} based on the value obtained from testing. For example, as shown in Fig. 3(a), the R_{on} of the SiC MOSFET stays constant at any current level, but varies with the temperature. Thus, it can be presented as a polynomial function of temperature, whose parameters can be extracted from test values by performing curve fitting. The test result of $R_{on,M}$ of the SiC MOSFET and its polynomial are shown in Fig. 7. Similar mathematical expressions can be obtained for the diodes and the IGBT, which are based on manufacturer values [22], [23]. Because of the limited data points, the linear models based on the data at two different temperatures are used for Si devices.

As shown in Fig. 6, the switching energy loss of the SiC MOSFET is a function of the current, and its change with temperature is negligible. Thus, it can be expressed as a polynomial function of current by performing curve fitting:

$$E(i) = 0.8468i^3 + 10.693i^2 + 6.0128i \ \mu\text{J}. \tag{4}$$

Then, the effective switching power loss for an SPWM-controlled inverter is expressed as:

$$P_{sw} = f_{sw} \cdot \frac{1}{2\pi} \int_{\phi}^{2\pi+\phi} E\left[i(\theta)\right] d\theta$$

$$= f_{sw} \cdot (0.1797I^3 + 2.6733I^2 + 1.9139I) \ \mu\text{W}. \tag{5}$$

The same method can be applied to diodes and IGBTs.

E. Thermal Models

The equivalent thermal circuit shown in Fig. 8 is used to analyze the thermal response of the converter [17], [18]. It can be solved in the frequency domain. The transfer functions are shown as follows:

$$Z_{jjc}(s) = \frac{R_{jj1}}{1+s\tau_{jj1}} + \frac{R_{jj2}}{1+s\tau_{jj2}} + \cdots + \frac{R_{jjn}}{1+s\tau_{jjn}} \tag{6}$$

$$Z_{djc}(s) = \frac{R_{dj1}}{1+s\tau_{dj1}} + \frac{R_{dj2}}{1+s\tau_{dj2}} + \cdots + \frac{R_{djn}}{1+s\tau_{djn}} \tag{7}$$

$$Z_{ca}(s) = \frac{R_{ch}}{1+s\tau_{ch}} + \frac{R_{ha}}{1+s\tau_{ha}}. \tag{8}$$

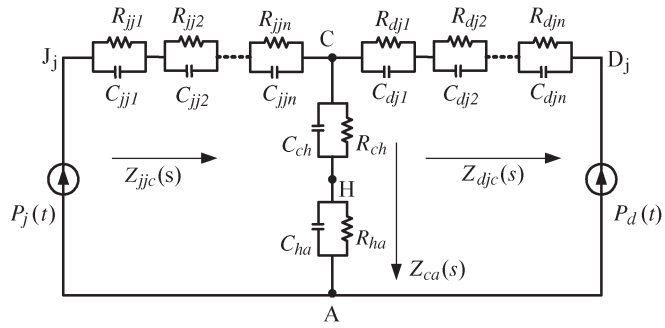

Fig. 8. Thermal equivalent circuit of an inverter.

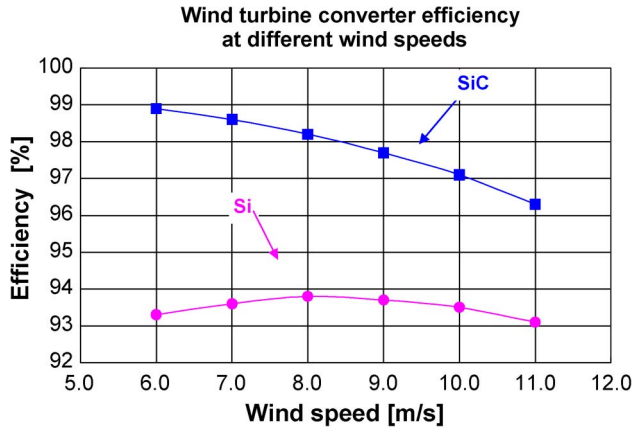

Fig. 9. Efficiency of SiC- and Si-based wind turbine converters at different wind speeds and 3 kHz switching frequency.

In (6)–(8), R is the thermal resistance and τ is the thermal time constant. Manufacturer data is used in the simulations.

III. Simulations and Discussions

The simulation of this wind generation system is done for wind speeds ranging from 6 to 11 m/s, which has the best energy density for modern wind turbines. Different switching frequencies are also studied. The junction temperature limit for both the Si and SiC systems is assumed to be 150 °C for Case A (switching frequency of 3 kHz) and Case B (switching frequency varies from 1 kHz to 50 kHz). In order to do a fair comparison, the power losses of the SiC MOSFETs are scaled corresponding to the rated voltage ratios of the SiC MOSFET and the Si IGBT (see Table II). In other words, the on-state resistance and switching loss used in the model assume that 1700-V devices were used for the SiC MOSFETs and Si IGBTs.

A. At Switching Frequency of 3 kHz

Currently, most commercial wind turbine converters are switched at frequencies around 3 kHz. The generator is designed to work at rated power at the wind speed of 11 m/s. By simulation, from 6 to 11 m/s, the converter efficiency (including the rectifier, inverter, and the power loss of the filter shown in Fig. 1) is shown in Fig. 9. At the whole speed range, the efficiency of the Si converter is lower than that of the SiC converter. More specifically, the average efficiency of the SiC converter is 97.8%, compared to 93.5% of the Si converter. If

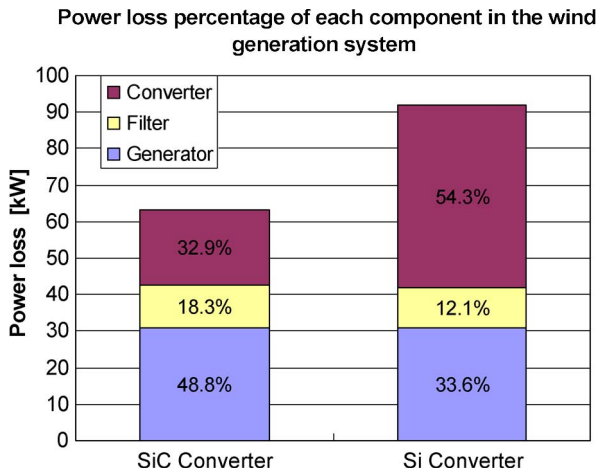

Fig. 10. Average power losses of the wind turbine system when using Si and SiC converters at 3 kHz at full power rating.

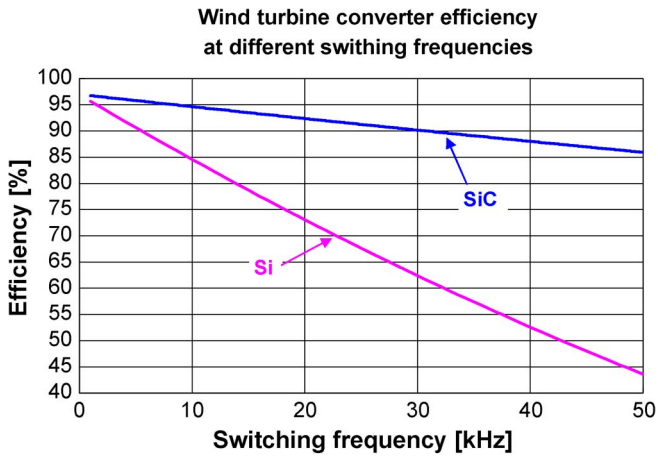

Fig. 11. Efficiency of SiC and Si wind turbine converters at full power rating and different switching frequencies.

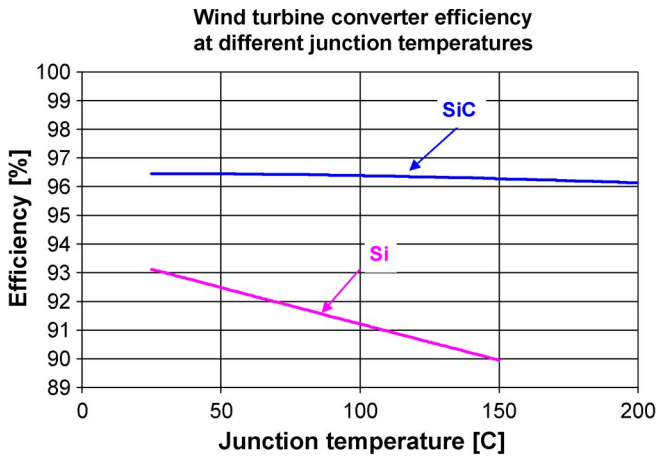

Fig. 12. Efficiency of SiC and Si wind turbine converters at full power rating and different temperatures.

power-loss saving of the SiC device compared to that of the Si device is defined by the difference of the power losses in the two devices over the power loss of the Si device, the average power loss saved by the SiC converter in this application is about 58.4%. In the worst case (wind speed at 11 m/s), it is about 43.2 kW.

The average power loss of each component in the two wind power generation systems is shown in Fig. 10. The efficiencies of the generators in the two systems are the same (96.4% on average), whether the Si or the SiC converter is used. However, for the Si-based system, the converter loss accounts for the most loss, which is as large as 54.3% (compared to 32.9% of the SiC-based system). Thus, it is necessary to reduce the loss in the converter in order to improve the generation system efficiency. The SiC converter is a good alternative.

B. At Frequency Up to 50 kHz

The power loss of the filter also accounts for a substantial portion in the total system loss for both converters (12.1% for Si-based versus 18.3% for the SiC-based system in Fig. 10). The size and loss of the filter are related to the switching frequency of the inverter. Increasing the switching frequency of the inverter can reduce the size and loss of the filter, and thus, the cost. Because high switching frequency capability is one of the merits of SiC devices, an analysis was made to consider the option of increasing the switching frequency of the converter in this application.

As shown in Fig. 11, as frequency increases from 1 to 50 kHz, the efficiency of the SiC converter (not including filter loss) at rated power and 25 °C ambient temperature linearly decreases at a rate of 1.1% per 5 kHz, and that of the Si converter decreases much more quickly at a rate of about 4.9% per 5 kHz.

In practice, the switching frequency of a large power electronic Si IGBT cannot exceed a few kiloHertz because of the large amount of loss. In this case, the efficiency of the Si converter at 20 kHz is 73.1%, which is not acceptable. While for the SiC converter, it has a relatively high efficiency of 85.9%, even at 50 kHz. Thus, it is possible to improve efficiency and reduce the cost of the system at the same time by using the SiC converter.

For example, by increasing the switching frequency of the SiC converter to 6 kHz, its efficiency will be 95.6%, which is the same as the efficiency of the Si converter switching at only 3 kHz, and at the same time, the size, loss, and cost of the filter are reduced for the SiC-based converter because of the 2× higher switching frequency.

C. High Temperature Capability of SiC Converter

When operating at full power rating and using a switching frequency of 3 kHz, the efficiency of the SiC converter decreases by only 0.2%, from 25 °C to 150 °C, as shown in Fig. 12. However, the efficiency of the Si converter is lowered by 3.2%, from 25 °C to 150 °C (see Fig. 12). Moreover, the efficiency of the SiC converter is higher for the tested temperature range, and the efficiency difference is greater at higher temperature. For example, the efficiency of the SiC converter is 6.3% higher than that of the Si converter at 150 °C.

Therefore, the cooling requirement of the SiC converter can be less than that of the Si converter, even with the same junction temperature limit. For example, the junction temperature limit

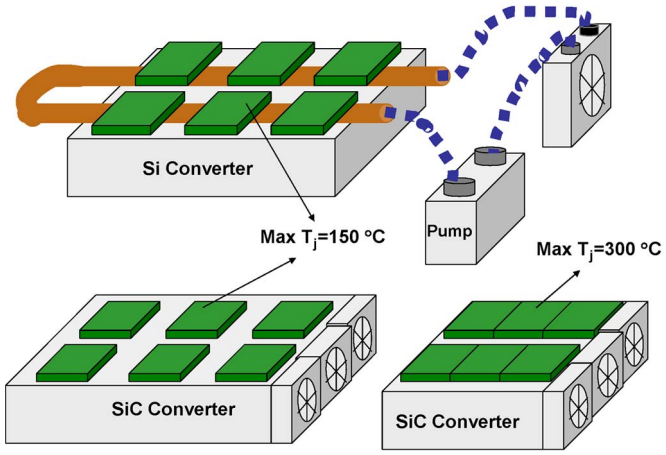

Fig. 13. Cooling system of Si and SiC converters.

for all devices is chosen to be 150 °C. As calculated by the simulation, the thermal resistance of the heatsinks required by the SiC converter is 0.11 K/W, assuming that the rectifier and inverter of each back-to-back converter are mounted separately on two heatsinks with the same thermal resistance value, and totally there are ten such converters. The value of 0.11 K/W can be realized by a natural or forced convection heatsink. To illustrate the size of the heatsink, a commercial heatsink product MF18-1515 from Conrad Engineering [24] is selected but may not be the best. The required thermal resistance can be achieved by forced cooling at an air flow rate of 27 cfm (12.7 l/s). Then, the approximate volume of the heatsinks, not including the cooling fans, is 23 480 cm^3.

Similarly, the thermal resistance of the heatsinks required by the Si converter is 0.0035 K/W, assuming that all the devices of each back-to-back converter are distributed equally on the same heatsinks with the same thermal resistance value, and totally there are two such converters. Liquid cooling is needed to achieve such low values. If the Hi-Contact liquid cold plates from Aavid Thermalloy, LLC [25] are used, the volume of the heatsinks will be about 24 278 cm^3 (and this does not include any accessories such as pumps, tubing, radiator, etc.). If the space occupied by the accessories is considered, the total volume of the Si converter would be much larger than that of the SiC one. Besides, the cooling management of the SiC converter is much simpler, as shown in Fig. 13, and less expensive. Based on the current market prices for the two kinds of heatsinks used here, the cost of the heatsinks for the SiC converter is about 1/8 of that for the Si converter.

Furthermore, SiC devices can work at higher temperatures (at least 300 °C junction temperature) with proper packaging. This can further reduce the size of the heatsinks. By simulation, the required thermal resistance of the SiC converter can be increased to 0.18 K/W under the same assumptions. If using the same series of heatsink products and forced cooling conditions, the thermal results value can be realized by MF18-75, which has a shorter length compared to MF18-1515. The approximate volume of the heatsinks, not including cooling fans, will be 11 624 cm^3 (about 49.5% of that with 150 °C temperature limit). The SiC converter with a smaller heatsink is also drawn in proportion to the other designs in Fig. 13.

IV. Conclusion

The simulations in this work has lead to a conclusion that the application of a SiC converter in the wind generation system will improve the system's efficiency, provide more output power, and reduce the system's size and cost due to the low-loss, high-frequency, and high-temperature properties of SiC devices even for one-for-one replacement. More benefits can be obtained by elevating the rated voltage of the system in order to take advantage of the high voltage capability of SiC devices. For any of these benefits to appear in a wind generation system, however, will require that manufacturers of SiC switching devices be able to produce sufficient quantities at costs that can show an overall system cost savings in installed cost and/or operating costs of the wind turbines.

References

[1] E. Echenique, J. Dixon, R. Cardenas, and R. Pena, "Sensorless control for a switched reluctance wind generator, based on current slopes and neural networks," *IEEE Trans. Ind. Electron.*, vol. 56, no. 3, pp. 817–825, Mar. 2009.

[2] B. Ni and C. Sourkounis, "Investigations on control methods for variable speed wind energy converters at strongly fluctuating wind power," in *Proc. IEEE Ind. Electron. Conf.*, Nov. 10–13, 2008, pp. 241–246.

[3] A. Mirecki, X. Roboam, and F. Richardeau, "Architecture complexity and energy efficiency of small wind turbines," *IEEE Trans. Ind. Electron.*, vol. 54, no. 1, pp. 660–670, Feb. 2007.

[4] A. G. Abo-Khalil and D.-C. Lee, "MPPT control of wind generation systems based on estimated wind speed using SVR," *IEEE Trans. Ind. Electron.*, vol. 55, no. 3, pp. 1489–1490, Mar. 2008.

[5] G. O. Cimuca, C. Saudemont, B. Robyns, and M. M. Radulescu, "Control and performance evaluation of a flywheel energy-storage system associated to a variable-speed wind generator," *IEEE Trans. Ind. Electron.*, vol. 53, no. 4, pp. 1074–1085, Jun. 2006.

[6] H. Li, M. Steurer, K. L. Shi, S. Woodruff, and D. Zhang, "Development of a unified design, test, and research platform for wind energy systems based on hardware-in-the-loop real-time simulation," *IEEE Trans. Ind. Electron.*, vol. 53, no. 4, pp. 1144–1151, Jun. 2006.

[7] S. Karimi, A. Gaillard, P. Poure, and S. Saadate, "FPGA-based real-time power converter failure diagnosis for wind energy conversion systems," *IEEE Trans. Ind. Electron.*, vol. 55, no. 12, pp. 4299–4308, Dec. 2008.

[8] R. C. Portillo, M. M. Prats, J. I. Leon, J. A. Sanchez, J. M. Carasco, E. Galvan, and L. G. Franquelo, "Modeling strategy for back-to-back three-level converters applied to high-power wind turbines," *IEEE Trans. Ind. Electron.*, vol. 53, no. 5, pp. 1483–1491, Oct. 2006.

[9] S. Zhang, K. J. Tseng, and T. D. Nguyen, "Modeling of AC-AC matrix converter for wind energy conversion system," in *Proc. IEEE Conf. Ind. Electron. Appl.*, May 25–27, 2009, pp. 184–191.

[10] M. Van Dessel and G. Deconinck, "Power electronic grid connection of PM synchronous generator for wind turbines," in *Proc. IEEE Ind. Electron. Conf.*, Nov. 10–13, 2008, pp. 2200–2205.

[11] J. B. Casady, *SiC Power Device Development for Clean Energy Application*, Sep. 2008. [Online]. Available: http://www.sandia.gov/ess/Publications/Conferences/2008/PR08_Presentations/ritenour_semisouth.pdf

[12] R. H. Wolk, *Proceedings of High Megawatt Power Converter Technology R&D Roadmap Workshop*, Apr. 2008. [Online]. Available: http://www.nist.gov/eeel/high_megawatt/upload/RoadadmapworkshopProceedingsFinal8-clean-al-1.pdf

[13] H. Zhang and L. M. Tolbert, "SiC's potential impact on the design of wind generation system," in *Proc. IEEE Ind. Electron. Conf.*, Nov. 10–13, 2008, pp. 2231–2235.

[14] G. Bywaters, V. John, J. Lynch, P. Mattila, G. Norton, J. Stowell, M. Salata, O. Labath, A. Chertok, and D. Hablanian, "Northern power systems WindPACT drive train," Subcontractor Rep. NREL/SR-500-35524, Apr. 2001–Jan. 2005. [Online]. Available: http://www.nrel.gov/wind/pdfs/35524.pdf

[15] D. A. Marckx, "Breakthrough in Power Electronics From SiC," Subcontractor Rep. NREL/SR-500-38515, May 2004–May 2005. [Online]. Available: http://www.nrel.gov/wind/pdfs/38515.pdf

[16] J. S. Lai, R. W. Young, G. W. Ott, Jr., and J. W. McKeever, "Efficiency modeling and evaluation of a resonant snubber based soft-switching inverter for motor drive applications," in *Proc. IEEE Power Electron. Spec. Conf.*, Jun. 18–22, 1995, pp. 943–949.
[17] M. H. Bierhoff and F. W. Fuchs, "Semiconductor losses in voltage source and current source IGBT converters based on analytical derivation," in *Proc. IEEE Power Electron. Spec. Conf.*, 2004, pp. 2836–2842.
[18] F. Blaabjerg, U. Jaeger, and S. Munk-Nielsen, "Power losses in PWM-VSI inverter using NPT or PT IGBT devices," *IEEE Trans. Power Electron.*, vol. 10, no. 3, pp. 358–367, May 1995.
[19] B. Ozpineci, L. M. Tolbert, S. K. Islam, and M. Hasanuzzaman, "Effects of silicon carbide (SiC) power devices on PWM inverter losses," in *Proc. IEEE Ind. Electron. Conf.*, Nov. 2001, pp. 1061–1066.
[20] H. Zhang, "Electro-thermal modeling of SiC power electronic systems," Ph.D. dissertation, Univ. Tennessee, Knoxville, TN, 2007.
[21] H. Zhang, L. M. Tolbert, B. Ozpineci, and M. Chinthavali, "A SiC-based converter as a utility interface for a battery system," in *Conf. Rec. IEEE IAS Annu. Meeting*, Oct. 8–12, 2006, pp. 346–350.
[22] *Datasheet of Silicon Carbide Schottky Diode-C2D10120*. [Online]. Available: www.cree.com/products/pdf/C2D10120.pdf
[23] *Datasheet of Silicon IGBT Module—DIM1600FSM17*. [Online]. Available: www.dynexsemi.com/assets/IGBT_Modules/Datasheets/DNX_DIM1600FSM17-A000.pdf
[24] *Conrad Heatsink 2005 Catalog*. [Online]. Available: http://www.conradheatsinks.com
[25] *Manufaturer Page of Hi-Contact Liquid Cold Plates From Aavid Thermalloy*, LLC. [Online]. Available: www.aavidthermalloy.com/products/liquid/hi-contact.pdf
[26] Y. Sugawara, D. Takayama, K. Asano, S. Ryu, A. Miyauchi, S. Ogata, and T. Hayashi, "4H-SiC high power SIJFET module," in *Proc. IEEE 15th Int. Symp. Power Semicond. Devices ICs*, Apr. 14–17, 2003, pp. 127–130.
[27] T. E. Salem, D. P. Urciuoli, R. Green, and G. K. Ovrebo, "High-temperature high-power operation of a 100 A SiC DMOSFET module," in *Proc. IEEE Appl. Power Electron. Conf. Expo.*, Feb. 15–19, 2009, pp. 653–657.
[28] J. M. Ortiz-Rodriguez, M. Hernandez-Mora, T. H. Duong, S. G. Leslie, and A. R. Hefner, "Thermal network component models for 10 kV SiC power module packages," in *Proc. IEEE Power Electron. Spec. Conf.*, Jun. 15–19, 2008, pp. 4770–4775.
[29] *Cree and Powerex Develop New SiC Power Switches for Next-Generation Military Systems*, Feb. 17, 2009. Press release of Cree, Inc., Durham N.C. [Online]. Available: www.cree.com/press/press_detail.asp?i=1234879464387
[30] T. Nezu, *Rohm exhibits new SiC power module*, Tech-on Newsletter, Oct. 16, 2009. [Online]. Available: http://techon.nikkeibp.co.jp/english/NEWS_EN/20091016/176491/

Hui Zhang (S'03–M'07) received the B.S. and M.S. degrees in electrical engineering from the Zhejiang University, Hangzhou, China, in 2000 and 2003, respectively, and the Ph.D. degree in electrical engineering from The University of Tennessee, Knoxville, in 2007.

She joined the Power Electronics and Electric Machinery Research Center at the Oak Ridge National Laboratory (ORNL), Knoxville, TN, as a student member in 2005. She was a Postdoctoral Research Associate at The University of Tennessee and at the Oak Ridge National Laboratory from 2007 until 2009. Currently, she is an Assistant Professor with the Electrical Engineering Department of Tuskegee University, Alabama.

Dr. Zhang is a member of IEEE Power Electronics Society, Industry Application Society, and the Industrial Electronics Society. She has served as a Reviewer of IEEE Transactions and the Session Chair of IEEE conferences.

Leon M. Tolbert (S'88–M'91–SM'98) received the Bachelor's, M.S., and Ph.D. degrees in electrical engineering from the Georgia Institute of Technology, Atlanta, in 1989, 1991, and 1999, respectively.

He was with the Engineering Division, Oak Ridge National Laboratory (ORNL), Knoxville, TN, in 1991. He was an Assistant Professor with the Department of Electrical and Computer Engineering, The University of Tennessee, Knoxville, in 1999. He is currently the Min Kao Professor with the Min Kao Department of Electrical Engineering and Computer Science, The University of Tennessee. He is also a Research Engineer with the Power Electronics and Electric Machinery Research Center, Oak Ridge National Laboratory.

Dr. Tolbert is a Registered Professional Engineer in the state of Tennessee. He is the recipient of an NSF CAREER Award in 2001, the 2001 IEEE Industry Applications Society Outstanding Young Member, and three prize paper awards from the IEEE Industry Applications Society and IEEE Power Electronics Society. From 2003 to 2006, he was the Chairman of the Education Activities Committee of the IEEE Power Electronics Society and an Associate Editor for the IEEE POWER ELECTRONICS LETTERS. He has been an Associate Editor of the IEEE TRANSACTIONSON POWER ELECTRONICS since 2007. He was elected as a Member-At-Large to the IEEE Power Electronics Society Advisory Committee for 2010–2012.